

# The Denitridation of Nitrides of Iron, Cobalt and Rhenium Under Hydrogen

A.-M. Alexander · J. S. J. Hargreaves ·  
C. Mitchell

© The Author(s) 2013. This article is published with open access at Springerlink.com

**Abstract** The denitridation behaviour of binary iron, cobalt and rhenium nitrides under  $H_2/Ar$  has been investigated. The iron nitride was found to lose over 70 % of its as prepared nitrogen content at 400 °C. The cobalt nitride was completely denitrided at 250 °C. Rhenium nitride lost close to 90 % of its nitrogen at 350 °C. In addition,  $Co-Re_4$  prepared by ammonolysis was investigated, whilst only traces of  $NH_3$  were lost from this material under  $H_2/Ar$  at 400 °C, with  $H_2/N_2$  it proved to be an active ambient pressure ammonia synthesis catalyst in accordance with previous literature.

**Keywords** Ammonia · Nitrogen · Rhenium · Cobalt · Iron · Nitride · Hydrogen

## 1 Introduction

Metal nitrides constitute an interesting class of heterogeneous catalyst [1–4]. In some cases their activities reportedly rival, or even exceed, those of commercial catalysts and comparisons between the efficacy of certain metal nitrides with that of noble metals have frequently been drawn in the

literature. With the aim of developing novel nitrogen transfer pathways, it is of interest to explore the reactivity of the lattice nitrogen within nitrides. This idea has its origins in the Mars-van Krevelen mechanism wherein oxidation over metal oxide catalysts is accomplished by the direct reaction of lattice oxygen with the substrate, and its subsequent replenishment from the gas phase oxidant [5]. This mechanism can also be developed into a two step process where the oxidation of substrate and the re-oxidation of reduced catalyst are performed in separate steps which can deliver selectivity and heat transfer advantages when the target product is, e.g., susceptible to further oxidation in the gas-phase. The selective oxidation of butane to yield maleic anhydride provides an example of a catalytic process for which such a two-stage procedure has been investigated [6]. In addition to oxidation reactions catalysed by metal oxides, Mars-van Krevelen-like reaction mechanisms are documented for other types of reaction [7], for example those involving sulfide [8] and carbide [9, 10] catalysts. In the case of carbides, it is interesting to note that a two stage process, methane decomposition to yield intermediate carbide and subsequent hydrogenation to yield higher hydrocarbons at lower temperature, has been employed for methane homologation [11, 12].

It is of interest to explore the possibility of utilising the reactivity of lattice nitrogen to develop novel nitrogen transfer pathways to generate products of industrial importance. If the replenishment of nitrogen depleted phases can be accomplished by  $N_2$  directly, more direct routes bypassing ammonia, which is often employed in large scale processes, may become available. This would be a significant development, especially when the energy intensive nature of ammonia synthesis [13] is taken into account. To date, such approaches seem to have been relatively little explored. Itoh et al. [14] have reported the production of

---

A.-M. Alexander · J. S. J. Hargreaves (✉)  
WestCHEM, School of Chemistry, Joseph Black Building,  
University of Glasgow, Glasgow G12 8QQ, UK  
e-mail: Justin.Hargreaves@glasgow.ac.uk

*Present Address:*  
A.-M. Alexander  
Department of Chemical and Biochemical Engineering, The  
Ohio State University, 140W 19th Ave, Columbus, OH 43210,  
USA

C. Mitchell  
Huntsman Polyurethanes, Everslaan 45, B-3078 Everberg,  
Belgium

ammonia by reduction from nitrogen-containing intermetallic phases generated by ammonolysis. Ley et al. [15–17] have employed magnesium nitride as a source of ammonia for organic synthesis in the presence of protic solvents. Aluminium nitride has also been used for this purpose [18]. The reactivity of lattice nitrogen to hydrolysis has also been investigated with the aim of applying solid phase metal nitride reactants to solar ammonia production [19]. The reactivity of binary and ternary molybdenum nitrides to hydrogen has been explored [20, 21]. Of particular note is the observation that 50 % of the lattice nitrogen can be removed from  $\text{Co}_3\text{Mo}_3\text{N}$  to yield  $\text{Co}_6\text{Mo}_6\text{N}$  which possesses a previously unprecedented structure wherein the residual nitrogen relocates from the 16c to 8a Wyckoff site [22, 23]. Furthermore, it is possible to regenerate  $\text{Co}_3\text{Mo}_3\text{N}$  by treatment of  $\text{Co}_6\text{Mo}_6\text{N}$  with  $\text{N}_2$  alone [24]. Similar experiments undertaken with molybdenum oxycarbonitrides have demonstrated that the reactivity of their lattice nitrogen is much greater than that of their lattice carbon [25].

Previously, we have reported upon the reactivity of the lattice nitrogen within  $\text{Cu}_3\text{N}$ ,  $\text{Ni}_3\text{N}$ ,  $\text{Zn}_3\text{N}_2$  and  $\text{Ta}_3\text{N}_5$  [26].  $\text{Cu}_3\text{N}$  and  $\text{Ni}_3\text{N}$  were found to be relatively unstable with up to 30 % of their lattice nitrogen generating  $\text{NH}_3$  at 250 °C, 15 % of the total lattice N available within  $\text{Zn}_3\text{N}_2$  yielded  $\text{NH}_3$  at 400 °C and in the case of  $\text{Ta}_3\text{N}_5$  reactivity of lattice N was definitely established with 13 % yielding  $\text{NH}_3$  up to 700 °C. In the present manuscript, we detail the reactivity of binary nitrides of iron, cobalt and rhenium to hydrogen as an initial screen to identify systems/conditions of potential interest for application. Renitridation of systems of interest, ideally by  $\text{N}_2$  alone, would be a necessary step in any envisaged application.

## 2 Experimental

Nitrides were prepared by ammonolysis. Approximately 0.5 g of each precursor was in a vertical quartz glass reactor into which 94 ml  $\text{min}^{-1}$  of  $\text{NH}_3$  (BOC, 99.98 %) was introduced. The furnace was programmed to heat the material in accordance with the conditions detailed below. Following reaction, the material was cooled under the flow of ammonia and, upon reaching ambient temperature, the system was purged with 100 ml  $\text{min}^{-1}$  of  $\text{N}_2$  gas (BOC, 99.995 %) for 30 min. In order to limit the possibility of their decomposition upon storage, both iron nitride and cobalt rhenium nitride samples were passivated using a mixture of 2 %  $\text{O}_2/\text{Ar}$  flowing at 5 ml  $\text{min}^{-1}$  and  $\text{N}_2$  flowing at 95 ml  $\text{min}^{-1}$ .

The precursors and conditions which were applied were based upon the previous literature and were as follows:

Iron nitride was prepared by the reaction of ammonia with Fe powder (Sigma Aldrich, 99+ %) at 500 °C for 6 h.

A temperature programmed ramp rate of 5 °C  $\text{min}^{-1}$  was employed and the sample was passivated as detailed above.

Cobalt nitride was prepared by reaction of ammonia with  $\text{Co}_3\text{O}_4$  at 700 °C for 2 h. The temperature was increased from room temperature to 300 °C over 30 min, after which it was increased to 450 °C at a rate of 0.7 °C  $\text{min}^{-1}$  and then up to 700 °C at a rate of 1.67 °C  $\text{min}^{-1}$ .

Rhenium nitride was prepared by ammonolysis of  $\text{NH}_4\text{ReO}_4$  (Sigma Aldrich, 99.5 %) at 350 °C for 2 h. A temperature ramp rate of 5 °C  $\text{min}^{-1}$  was applied.

Cobalt rhenium nitride was prepared by ammonolysis of a cobalt rhenium oxide precursor at 700 °C for 3 h. A temperature ramp rate of 5 °C  $\text{min}^{-1}$  was applied. The sample was passivated as detailed above. The precursor was prepared by incipient wetness impregnation of  $\text{NH}_4\text{ReO}_4$  with  $\text{Co}(\text{NO}_3)_2 \cdot 6\text{H}_2\text{O}$  (Sigma Aldrich, 98+ %) to yield a Co/Re ratio of 1/4. The sample was dried overnight and calcined in air at 500 °C for 3 h.

The reduction of samples was undertaken using a 60 ml  $\text{min}^{-1}$  flow of a 1/3  $\text{Ar}/\text{H}_2$  (BOC,  $\text{H}_2$  99.998 %,  $\text{Ar}$  99.99 %) mixture. In each case, ~0.3 g of material was placed in a quartz microreactor and held between quartz wool plugs centrally in the heated zone of a tube furnace. Ammonia production was determined by measurement of the decrease in conductivity of a 200 ml 0.0018 M  $\text{H}_2\text{SO}_4$  solution through which the reactor effluent stream was flowed. In those instances where the amount of ammonia produced made it necessary to use more than one flask of 0.0018 M  $\text{H}_2\text{SO}_4$  solution, the conductivity is reported in arbitrary units (a.u.). The proportion of ammonia produced as a function of the total change of nitrogen content upon reaction is reported as a percentage. The initial nitrogen content for samples corresponds to that determined from elemental analysis following preparation (and subsequent passivation in the case of the iron and cobalt rhenium samples.) Comparative measurements of the ammonia synthesis efficacy were undertaken under similar conditions using a 1/3  $\text{N}_2/\text{H}_2$  gas mixture (BOC  $\text{H}_2$  99.998 %,  $\text{N}_2$  99.99 %) instead of 1/3  $\text{Ar}/\text{H}_2$ . The temperature conditions for which sample reduction and ambient pressure ammonia synthesis testing was measured are described in Sect. 3. In the case of the previously passivated iron and cobalt rhenium materials, the resultant oxide layer was removed in situ prior to reaction with  $\text{Ar}/\text{H}_2$  and  $\text{N}_2/\text{H}_2$ , using a 1/3  $\text{N}_2/\text{H}_2$  gas mixture (BOC  $\text{H}_2$  99.998 %,  $\text{N}_2$  99.99 %) at 700 °C for 2 h. This does mean that there may be resultant differences in composition from those reported for the as-prepared passivated materials and this needs to be born in mind.

Powder XRD analyses were performed using a Siemens D5000 instrument operating with  $\text{CuK}_\alpha$  radiation (40 kV, 40 mA). A step size of 0.02° was applied with a counting

time of 1 s per step. Samples were prepared by compaction into a sample holder.

Nitrogen analysis was undertaken using an Exeter Analytical CE-440 Elemental Analyser. Analyses were performed in duplicate with reported accuracies of  $\pm 0.03$  wt%.

The surface area of materials was determined by application of the BET method to nitrogen physisorption isotherms which were determined at liquid nitrogen temperature on a Micromeritics Gemini instrument following degassing.

### 3 Results and Discussion

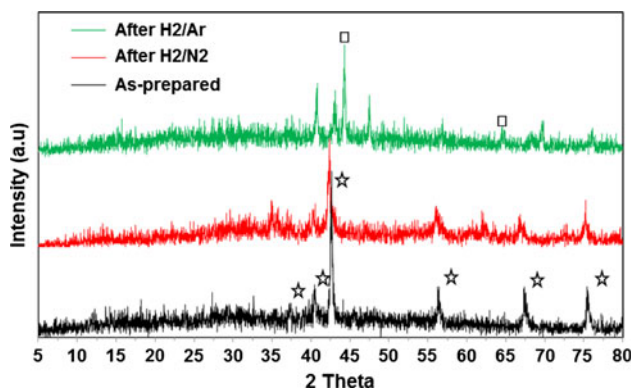
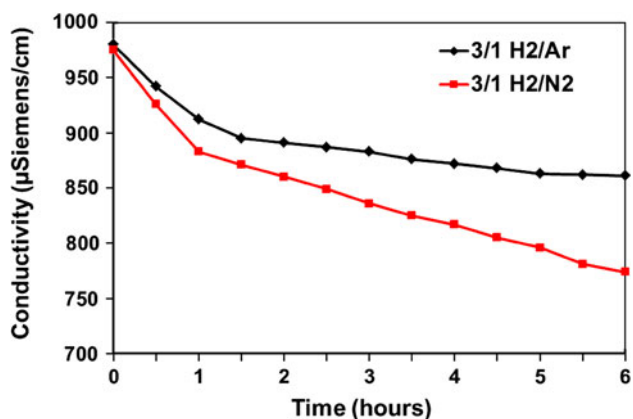
In early work, Goodeve and Jack [27] had investigated the denitridation of iron nitride by thermal decomposition, reduction with CO and reduction with  $H_2$ . It was reported that hydrogen enhanced the rate of nitrogen loss by four orders of magnitude compared to thermal decomposition and that the lattice nitrogen lost was completely converted to ammonia in the temperature range of 250–450 °C. Of particular relevance to the objective of developing nitrogen transfer reagents from nitrides was the observation that up to 25 % of the nitrogen lost by reaction with CO formed cyanogen with isomorphous substitution of lattice N by C also occurring. On this basis, it seems worthwhile to revisit binary iron nitride in the context of the current study. There has also been some recent interest in the application of binary iron nitrides as catalysts, where they have been reported to be effective hydrazine [28] and ammonia [29] decomposition catalysts and in  $SiO_2$  supported form active catalysts for the amination of ethylene with  $NH_3$  [30]. In the preparation of sponge-like  $Fe_3N$ , calcination under  $N_2$  was reported to be crucial to successfully generate the nitride phase [29]. The bulk structure of industrial ammonia synthesis catalysts is reportedly nitrided [31]. In the current study, the iron nitride was prepared by nitridation of iron metal with ammonia as described in the experimental section. The resultant nitrogen content, as determined by combustion analysis, is reported in Table 1. The stoichiometric N contents expected for  $Fe_2N$  and  $Fe_3N$ , two commonly reported phases, are expected to be 11.13 and 7.71 wt% respectively. It can be seen that the value reported in the Table lies between these two values implying that a material with an intermediate stoichiometry is formed. This is not unexpected, since a number of different phases of iron nitride have been documented and a range of stoichiometries are known to exist, e.g. [32, 33]. Powder X-ray analysis of the sample was performed and the diffractogram is reported in Fig. 1. Reasonable matches can be made to a number of the listed iron nitride patterns in the JCPDS index including 03-0910  $Fe_2N$ , 01-1236

$Fe_3N$ , 03-1174 zeta- $FeN$ , 03-0983  $Fe_2N$  and 06-0656  $Fe_2N$ . The relative intensity of the reflections is most consistent with 01-1236  $Fe_3N$  pattern. The positions of the reflections corresponding to this phase are shown in Fig. 1 where it can be seen that the reflections are shifted to lower  $2\theta$  values. This could be consistent with the formation of an  $\epsilon$ - $Fe_3N_{1+x}$  phase. It should also be noted that the overall intensity of the reflections is fairly low implying the possibility of a relatively high content of x-ray amorphous phase(s). Figure 2 shows the production of ammonia from this sample, as monitored by the decrease in conductivity of the standard  $H_2SO_4$  solution at the reactor exit, for the reaction of 3/1  $H_2/N_2$  and 3/1  $H_2/Ar$  at 400 °C in the presence of this sample. In both cases, there is a relatively sharp decrease in conductivity occurring in the initial 1 h on stream, which possibly corresponds to hydrogenation of surface  $NH_x$  groups formed on pretreatment. At longer times on stream an apparently steady state rate corresponding to ca.  $50 \mu mol h^{-1} g^{-1}$  is attained in the case of the  $H_2/N_2$  reaction, as might be expected for a catalytic reaction. In the case of  $H_2/Ar$  the diminution in conductivity is seen to be lower, which is consistent with the consumption of the sample's nitrogen by  $H_2$ . Post-reaction N analyses were undertaken and the results are reported in Table 1 in which it can be seen that the majority of the nitrogen has been lost from both samples, with the loss for  $H_2/N_2$  being lower as might be anticipated. The recovery of lost N as  $NH_3$  from the  $H_2/Ar$  treated sample corresponds to <10 % of the pre-activated sample N content. Post-reaction XRD analyses were undertaken and these are also shown in Fig. 1. It can be seen that there is, in general, an overall loss of crystallinity upon reaction. A number of other differences are apparent. The formation of Fe metal, as evidenced by reflections occurring at ca.  $45^\circ$  and ca.  $65^\circ$   $2\theta$  is apparent in the pattern of the  $H_2/Ar$  treated sample. Surprisingly, in view of its similar N content this phase is not evident in the pattern of the  $H_2/N_2$  treated sample. However, there are additional reflections which may correspond to lower binary nitrides such as  $Fe_4N$ . Given the drastic reduction, more significant changes in the post-reaction XRD patterns may have been anticipated. However, in this respect, as mentioned above, it is important to remember that there could be a significant fraction of XRD invisible phase present.

A very recent study has shown the generation of ammonia by hydrogenation of small cobalt nitride clusters of the form  $Co_mN$  (where  $m = 7, 8$  and  $9$ ) [34]. Accordingly, it is of interest to determine the reduction behaviour of binary cobalt nitrides. Within the literature, there have been only a few studies of the catalytic behaviour of cobalt nitrides. Amongst those reported, has been the application of supported  $Co_4N$  for preferential CO oxidation [35], NO decomposition [36] and hydrazine decomposition [37].

**Table 1** Pre- and post-reaction N content of binary iron nitride

Reactant mixture	Stoichiometric N content corresponding to Fe <sub>2</sub> N (wt%)	Pre-reaction N content (wt%)	Post-reaction N content (wt%)
H <sub>2</sub> /N <sub>2</sub>	11.13	8.65	3.57
Ar/H <sub>2</sub>	11.13	8.65	2.40

Pre-reaction BET surface area = 13 m<sup>2</sup> g<sup>-1</sup>**Fig. 1** XRD patterns of pre- and post-reaction iron nitride samples**Fig. 2** Conductivity profiles for the iron nitride samples reacted with 3/1 H<sub>2</sub>/N<sub>2</sub> and 3/1 H<sub>2</sub>/Ar at 400 °C

Fang et al. [38] have reported the stepwise decomposition of Co<sub>4</sub>N via Co<sub>3</sub>N to Co<sub>2</sub>N upon thermal annealing thin films of cobalt nitride. The preparation of cobalt nitride was found to be challenging with formation possibly only being achieved within a narrow temperature window. The method adopted was ammonolysis of Co<sub>3</sub>O<sub>4</sub> at 700 °C for 2 hours followed by cooling in NH<sub>3</sub>. The XRD pattern of the resultant phase is shown in Fig. 3. As has been discussed elsewhere [35–37], the strong similarity in the patterns for Co and Co<sub>4</sub>N makes unambiguous assignment extremely challenging. The pre-reaction N content (Table 2) demonstrates the presence of some nitrogen associated with the samples prepared in this manner, but the quantities are

significantly lower than would be expected for stoichiometric Co<sub>4</sub>N and there is variation between different batches. Therefore, in view of these uncertainties, it can not be definitively concluded that a bulk phase binary nitride, as opposed to Co metal containing sorbed NH<sub>x</sub> species, was formed. Nevertheless, it was still deemed of interest to determine the reduction characteristics of samples since the reaction of sorbed NH<sub>x</sub> species may still be useful in the development of two stage amination processes whereby ammonia is partly decomposed upon a surface in the first step and subsequently reacted by a target molecule in the second step. This type of process could be of value in those reactions where direct amination by NH<sub>3</sub> is thermodynamically limited by dehydrogenation, for example in the direct amination of benzene to yield aniline [39, 40]. To determine the overall stability of the resultant Co–N phase, temperature programmed reaction was undertaken as presented in Fig. 4. From this figure, it can be seen that the loss of NH<sub>3</sub> occurs within ca 1 h on stream at 250 °C and this corresponds to total loss of nitrogen from the sample as reported in Table 2. Hence, subsequent isothermal reactions were conducted using 3/1 H<sub>2</sub>/N<sub>2</sub> and 3/1 H<sub>2</sub>/Ar at this temperature. The results are presented in Fig. 5; Table 2 in which it can be seen that there may be a marginal effect of reaction atmosphere with the presence of N<sub>2</sub> possibly suppressing the loss of nitrogen. The quantity of ammonia produced as a proportion of N lost is around 13 % in the case of the H<sub>2</sub>/Ar reaction.

Rhenium nitride has been investigated for its ammonia synthesis activity and partial decomposition at 350 °C to yield a mixture of Re metal and Re<sub>3</sub>N was reported to occur resulting in a catalyst of higher activity than Re metal alone [41]. Denitridation of rhenium nitride was also observed during hydrodenitrogenation [42]. A number of studies have reported that Re based systems are active catalysts for ammonia synthesis [43–48]. Therefore, in view of the ability of Re to activate nitrogen and the apparent reactivity of lattice nitrogen in rhenium nitride, it was of interest to investigate this system further within the context of the current study. Rhenium nitride was prepared according to the method documented literature wherein ammonolysis of NH<sub>4</sub>ReO<sub>4</sub> was undertaken at 350 °C for 2 h [41]. The XRD pattern of the resultant material is presented in Fig. 6. Consistent with the literature [41, 42], the pattern consists of very broad reflections. Given that the surface area of this material was determined to be 2 m<sup>2</sup>g<sup>-1</sup>, which indicates the presence of large non-porous crystallites, it is likely that this effect is related to the occurrence of disorder. The nitrogen content of pre-reaction samples is reported in Table 3. It is generally found that rhenium nitride with a stoichiometry of around Re<sub>3</sub>N is formed when this preparation route is employed [41, 42]. Given that the theoretical nitrogen content of this phase equates to



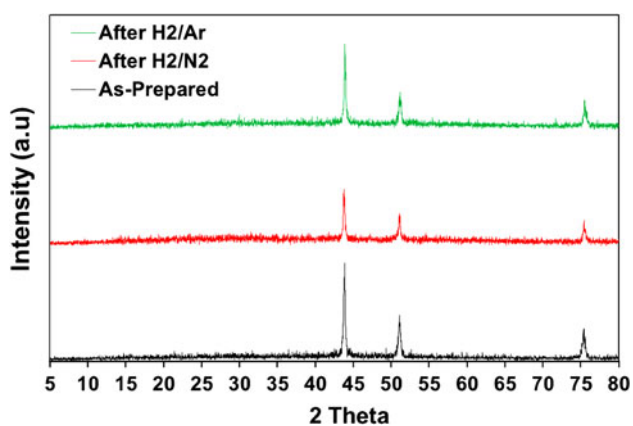


**Fig. 3** XRD patterns of pre- and post-reaction cobalt nitride samples

**Table 2** Pre- and post-reaction N content of cobalt samples

Reaction conditions	Stoichiometric N content corresponding to $\text{Co}_4\text{N}$ (wt%)	Pre-reaction N content (wt%)	Post-reaction N content (wt%)
$\text{H}_2/\text{Ar}$ temperature programme	5.60	3.17	0.00
$\text{H}_2/\text{Ar}$ (250 °C)	5.60	3.09	0.00
$\text{H}_2/\text{N}_2$ (250 °C)	5.60	3.39	0.89

Pre-reaction BET surface area = ca.  $4 \text{ m}^2 \text{ g}^{-1}$

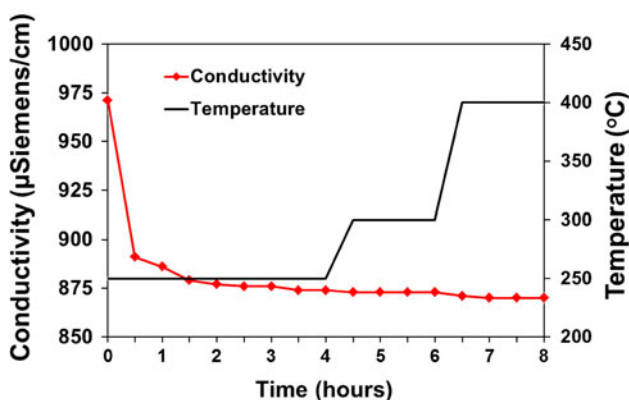


**Fig. 4** Temperature programmed conductivity profile for the cobalt nitride sample reacted with 3/1  $\text{H}_2/\text{Ar}$

2.44 wt%, it can be seen that the value determined is close to that which would be expected. Rhenium nitride reportedly decomposes to the metal above ca 370 °C [42]. Consequently, reduction of the sample employing 3/1  $\text{Ar}/\text{H}_2$  was undertaken using a temperature programme between 300 and 400 °C as reported in Fig. 7. From this figure, it can be seen that there is further loss of the sample's nitrogen at 350 °C, which is consistent with the ammonia synthesis study reported earlier [41]. The post-reaction XRD pattern of this material is consistent with the

presence of both reflections corresponding to Re metal and the broader reflections corresponding to the pre-reaction rhenium nitride phase (Fig. 6). Subsequently, the sample was further investigated at 350 °C where a comparison between the ammonia production efficacy under  $\text{H}_2/\text{Ar}$  and  $\text{H}_2/\text{N}_2$  was undertaken as shown in Fig. 8. From this figure, the greater degree of ammonia production in the presence of  $\text{H}_2/\text{N}_2$  can be seen, which is consistent with the known catalytic behaviour of this material. The rate of ammonia production in this sample corresponds to ca.  $130 \mu\text{mol h}^{-1} \text{ g}^{-1}$  (although steady state is not attained) which compares with the value of  $179 \mu\text{mol h}^{-1} \text{ g}^{-1}$  reported previously [41]. Both samples possess similar post-reaction N analyses with the  $\text{H}_2/\text{N}_2$  reacted sample, as may be expected, containing slightly more N—the greater degree of N loss in these samples as compared to the temperature programmed reacted samples may be attributed to the fact that they have spent longer at 350 °C or above (6 h for the isothermal runs vs. ca 4 h for the temperature programmed run.) They also possess similar XRD patterns which correspond to Re metal. The proportion of ammonia formed in the isothermal  $\text{H}_2/\text{Ar}$  treated sample corresponds to close to 30 % of the nitrogen content of the pre-reaction sample.

The inclusion of cobalt in nitrated rhenium catalysts has been reported to strongly improve ammonia synthesis activity, particularly when a material of composition  $\text{Co-Re}_4$  is prepared [41, 46]. Ammonolysis was conducted at much higher temperature (700 °C) and it was proposed that, despite the relatively low thermal stability of  $\text{Re}_3\text{N}$ , a rhenium nitride phase was formed. We have repeated the preparation and the powder XRD pattern of the resultant material is presented in Fig. 9. The features are consistent with those published previously [41] with the sharper reflections corresponding to Re and Co. Comparison of ammonia production at 400 °C for  $\text{H}_2/\text{N}_2$  and  $\text{H}_2/\text{Ar}$  feeds was undertaken and the results are presented in Fig. 10. A low level of ammonia, corresponding to ca.  $75 \mu\text{mol g}^{-1}$

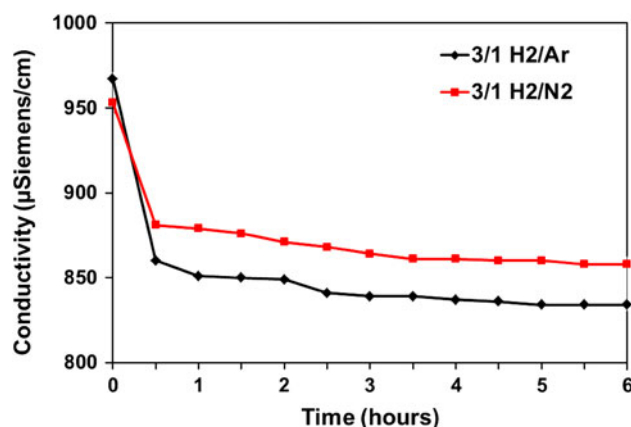


**Fig. 5** Conductivity profiles for the cobalt nitride samples reacted with 3/1  $\text{H}_2/\text{N}_2$  and 3/1  $\text{H}_2/\text{Ar}$  at 250 °C

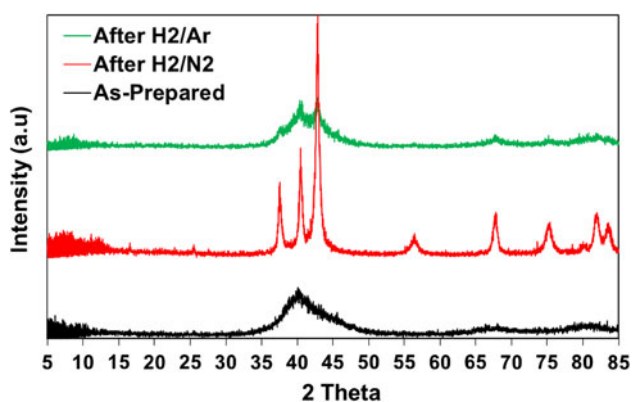


**Fig. 6** XRD patterns of the pre- and post-reaction rhenium nitride samples

**Table 3** Pre- and post-reaction N content of the rhenium nitride samples

Reaction conditions	Stoichiometric N content corresponding to $\text{Re}_3\text{N}$ (wt%)	Pre-reaction N content (wt%)	Post-reaction N content (wt%)
Ar/ $\text{H}_2$ temperature programme	2.44	2.46	1.10
Ar/ $\text{H}_2$ 350 °C	2.44	2.52	0.32
$\text{N}_2/\text{H}_2$ 350 °C	2.44	2.52	0.47

Pre-reaction BET surface area =  $2 \text{ m}^2 \text{ g}^{-1}$

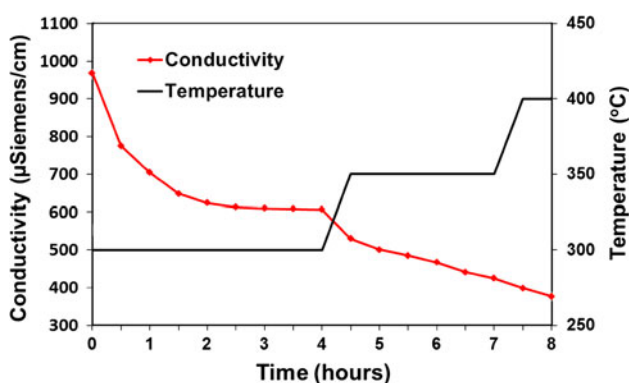


**Fig. 7** Temperature programmed conductivity profile for the rhenium nitride sample reacted with 3/1  $\text{H}_2/\text{Ar}$

was produced in the case of the  $\text{H}_2/\text{Ar}$  feed. In contrast, the  $\text{H}_2/\text{N}_2$  reaction generated ammonia corresponding to a steady state rate of  $472 \mu\text{mol h}^{-1} \text{ g}^{-1}$  (which compares with the  $600 \mu\text{mol h}^{-1} \text{ g}^{-1}$  reported at 350 °C reported elsewhere [41, 46]). Post-reaction XRD patterns indicate little change, aside from a possible increase in reflection intensities arising from increased crystallinity, occurring upon reaction.

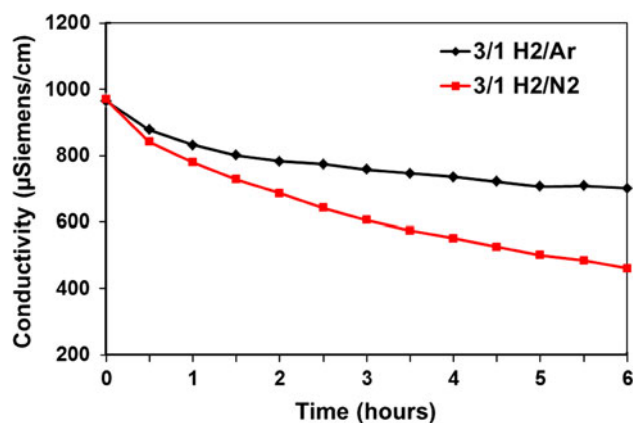


**Fig. 8** Conductivity profiles for the rhenium nitride samples reacted with 3/1  $\text{H}_2/\text{N}_2$  and 3/1  $\text{H}_2/\text{Ar}$  at 350 °C

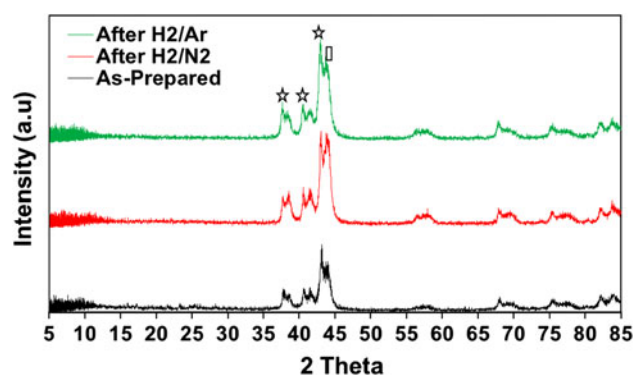


**Fig. 9** XRD patterns of pre- and post-reaction  $\text{Co-Re}_4$  samples (Co  $\square$ , Re  $\star$ )

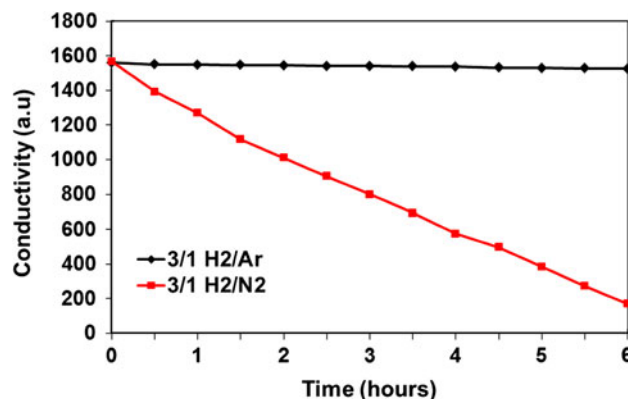


**Fig. 10** Conductivity profiles for the  $\text{Co-Re}_4$  samples reacted with 3/1  $\text{H}_2/\text{N}_2$  and 3/1  $\text{H}_2/\text{Ar}$  at 400 °C

## 4 Conclusions

The denitridation behaviour of nitrides of iron, cobalt and rhenium under an  $\text{Ar}/\text{H}_2$  atmosphere has been probed to determine the reactivity of lattice nitrogen as an initial screen for their potential application as nitrogen transfer

reagents. In all cases, ammonia was produced as a minor product, accounting for 10 % of the nitrogen content of the iron nitride studied at 400 °C, 13 % of that of cobalt nitride at 250 °C and 30 % of that of rhenium nitride at 350 °C. In addition, the ambient pressure ammonia synthesis activity of the materials using N<sub>2</sub>/H<sub>2</sub> has been investigated at the temperature of denitridation and the catalytic activity of the iron and rhenium systems, following an initial relatively sharp decline, possibly originating from hydrogenation of NH<sub>x</sub> species. The behaviour of nitrated Co-Re<sub>4</sub> was also investigated and whilst only very low levels of NH<sub>3</sub> formation under Ar/H<sub>2</sub> at 400 °C were apparent, its ambient pressure NH<sub>3</sub> synthesis was found to be significantly higher than all the other materials investigated.

**Acknowledgments** We would like to express our appreciation to Mrs Kim Wilson, University of Glasgow, for her very kind assistance in performing the nitrogen analyses. We also are very grateful to Huntsman Polyurethanes and the School of Chemistry, University of Glasgow for the provision of financial support.

**Open Access** This article is distributed under the terms of the Creative Commons Attribution License which permits any use, distribution, and reproduction in any medium, provided the original author(s) and the source are credited.

## References

- Furimsky E (2003) *Appl Catal A Gen* 240:1
- Nagai M (2007) *Appl Catal A Gen* 322:178
- Alexander A-M, Hargreaves JSJ (2010) *Chem Soc Rev* 39:4388
- Hargreaves JSJ (2013) *Coord Chem Rev* 257:2015
- Mars P, van Krevelen DW (1954) *Chem Eng Sci Spec Suppl* 41:263
- Contractor RM (1999) *Chem Eng Sci* 54:5627
- Doornkamp C, Ponc V (2000) *J Mol Catal A: Chem* 162:19
- Tetenyi P (2006) In: Hargreaves JSJ, Jackson SD, Webb G (eds) *Isotopes in heterogeneous catalysis*. Imperial College Press, London ISBN 978-1-86094-584-7 (Chapter 4)
- Garcia JM, Prinsloo FF, Niemantsverdriet JW (2009) *Catal Lett* 133:257
- Xiao T, Hanif A, York APE, Nishizaka Y, Green MLH (2002) *Phys Chem Chem Phys* 4:4549
- Koerts T, van Santen RA (1991) *J Chem Soc Chem Commun* 18:1281
- Koerts T, Deelen MJA, van Santen RA (1992) *J Catal* 138:101
- Bielawa H, Hinrichsen O, Birkner A, Muhler M (2001) *Angew Chemie Int Ed* 40:1061
- Itoh M, Machida K, Hirose K, Sakata T, Mori H, Adachi G (1999) *J Phys Chem B* 103:9498
- Veitch GE, Bridgwood KL, Ley SV (2008) *Org Lett* 10:3623
- Bridgwood KL, Veitch GE, Ley SV (2008) *Org Lett* 10:3627
- Veitch G E, Bridgwood K L, Rands-Trevor K, Ley S V (2008) *Synlett* 2597. DOI: 10.1055/s-0028-1083504
- Ghorbani-Choghmarani A, Zolfigol MA, Hajjami M, Goudarziafshar H, Nikoorazm M, Yousefi S, Tahmasbi B (2011) *J Braz Chem Soc* 22:525
- Michalsky R, Pfromm P (2012) *J Phys Chem C* 116:23243
- Mckay D, Hargreaves JSJ, Rico JL, Rivera JL, Sun XL (2008) *J Solid State Chem* 181:325
- Hargreaves JSJ, Mckay D (2009) *J Mol Catal A: Chem* 305:125
- Mckay D, Gregory DH, Hargreaves JSJ, Hunter SM, Sun X-L (2007) *Chem Commun* 29:3051
- Hunter SM, Mckay D, Smith RI, Hargreaves JSJ, Gregory DH (2010) *Chem Mater* 22:2898
- Gregory DH, Hargreaves JSJ, Hunter SM (2011) *Catal Lett* 141:22
- AlShalwi M, Hargreaves JSJ, Liggat JJ, Todd D (2012) *Mater Res Bull* 47:1251
- Alexander A-M, Hargreaves JSJ, Mitchell C (2012) *Top Catal* 55:1046
- Goodeve C, Jack KH (1948) *Disc Faraday Soc* 4:82
- Zheng MY, Chen XW, Cheng RH, Li N, Sun J, Wang XD, Zhang T (2006) *Catal Commun* 7:187
- Schnepf Z, Thomas M, Glatzel S, Schlichte K, Palkovits R, Giordano C (2011) *J Mater Chem* 21:17760
- Wang L, Xin Q, Zhao Y, Zhang G, Dong J, Gong W, Guo H (2012) *ChemCatChem* 4:624
- Schlögl R (2003) *Angew Chem Int Ed* 42:2004
- Pelka R, Arabczyk (2009) *Top Catal* 52:1506
- Liapina T, Leinenweber A, Mittemeijer EJ, Kockelmann W (2004) *Acta Mater* 52:173
- Yin S, Xie Y, Berntsein ER (2012) *J Chem Phys* 137:124304
- Yao Z, Zhang X, Peng F, Yu H, Wang H, Yang J (2011) *Int J Hyd Energy* 36:1955
- Yao Z, Zhu A, Chen J, Wang X, Au CT, Shi C (2007) *J Solid State Chem* 180:2635
- Cheng H, Huang Y, Wang A, Wang X, Zhang T (2009) *Top Catal* 52:1535
- Fang JS, Yang LC, Hsu CS, Chen GS, Lin YW (2004) *J Vac Sci Technol, A* 22:698
- Becker J, Holderich WF (1998) *Catal Lett* 54:125
- Desrosiers P, Guan SH, Hagemeyer A, Lowe DM, Lugmair C, Poorjary DM, Turner H, Weinburg H, Zhou XP, Armbrust R, Fengler G, Notheis U (2003) *Catal Today* 81:319
- Kojima R, Aika K-I (2001) *Appl Catal A Gen* 209:317
- Clark P, Dhandapani B, Oyama ST (1999) *Appl Catal A Gen* 184:L175
- Spencer ND, Somorjai GA (1982) *J Phys Chem* 86:3493
- Spencer ND, Somorjai GA (1982) *J Catal* 78:142
- Asscher M, Somorjai GA (1984) *Surf Sci* 143:L389
- Kojima R, Aika K-I (2000) *Chem Lett* 29(8):912
- Hayashi F, Iwamoto M (2011) *Microporous Mesoporous Materials* 146:184
- Kojima R, Enomoto H, Muhler M, Aika K-I (2003) *Appl Catal A Gen* 246:311